Breakdown of Migdal-Eliashberg theory; a determinant quantum Monte Carlo study

I. Esterlis¹, B. Nosarzewski^{1,2}, E. W. Huang^{1,2}, B. Moritz², T. P. Devereaux^{2,3}, D. J. Scalapino⁴, S. A. Kivelson^{1,3}

¹Department of Physics, Stanford University, Stanford, California 94305, USA

²Stanford Institute for Materials and Energy Sciences,

SLAC National Accelerator Laboratory and Stanford University, Menlo Park, CA 94025, USA

³Geballe Laboratory for Advanced Materials, Stanford University, Stanford, CA 94305, USA

⁴Department of Physics, University of California, Santa Barbara, CA 93106-9530, USA

The superconducting (SC) and charge-density-wave (CDW) susceptibilities of the two dimensional Holstein model are computed using determinant quantum Monte Carlo (DQMC), and compared with results computed using the Migdal-Eliashberg (ME) approach. We access temperatures as low as 25 times less than the Fermi energy, E_F , which are still above the SC transition. We find that the SC susceptibility at low T agrees quantitatively with the ME theory up to a dimensionless electron-phonon coupling $\lambda_0 \approx 0.4$ but deviates dramatically for larger λ_0 . We find that for large λ_0 and small phonon frequency $\omega_0 \ll E_F$ CDW ordering is favored and the preferred CDW ordering vector is uncorrelated with any obvious feature of the Fermi surface.

Introduction: The electron-phonon (e-p) problem is of broad importance in solid-state physics, and especially so in the theory of superconductivity (SC). In this context, a key question is what are the conditions that lead to the highest possible SC transition temperature, T_c . Given that this occurs when the dimensionless e-p coupling λ_0 is not small, one would a priori expect this question might be analytically unanswerable. However, Migdal-Eliashberg (ME) theory purports to be valid even if λ_0 is not small, provided $\lambda_0 \omega_0 / E_F$ is small, where ω_0 is an average phonon frequency and E_F is the Fermi energy [1, 2]. On the other hand, from a strong-coupling (large λ_0) perspective, it is clear ME theory breaks down for large λ_0 no matter how small ω_0/E_F , due to the formation of bipolarons [3-5]. Thus, one faces the practical question: at what value of the e-p coupling does ME theory break down, and how?

Model: To be explicit, we consider the two-dimensional Holstein Hamiltonian [6]

$$H = H_e + H_p + H_{ep},\tag{1}$$

where

$$H_e = -\sum_{ij,\sigma} t_{ij} (c_{i\sigma}^{\dagger} c_{j\sigma} + \text{h.c.}) - \mu \sum_{i,\sigma} n_{i\sigma},$$

$$H_p = \sum_i \left(\frac{P_i^2}{2M} + \frac{1}{2} K X_i^2 \right),$$

$$H_{ep} = \alpha \sum_{i,\sigma} n_{i,\sigma} X_i,$$
(2)

 $c_{i\sigma}^{\dagger}$ creates an electron on site i with spin polarization $\sigma = \uparrow, \downarrow$, $n_{i\sigma} = c_{i\sigma}^{\dagger} c_{i\sigma}$ is the local electronic density, P_i and X_i are the position and momentum operators of Einstein phonons with mass M, and μ is the chemical potential. The bare phonon frequency is thus $\omega_0 = \sqrt{K/M}$, and α is the e-p coupling constant. (We take units in which $M = \hbar = k_B = 1$.)

There are two important dimensionless parameters in

the model: the adiabatic parameter ω_0/E_F and the dimensionless e-p coupling

$$\lambda_0 = \alpha^2 \rho(E_F) / K,\tag{3}$$

where $\rho(E_F)$ is the density of states at the Fermi energy. To make contact with other approaches we also present data as a function of a "renormalized" coupling, denoted by λ , which we define in analogy with the phenomenological coupling extracted from tunneling spectra and often used in studies of "strongly-coupled" superconductors [7]. In the limit of weak coupling, $\lambda = \lambda_0 + \mathcal{O}(\lambda_0^2)$, but for $\lambda_0 \sim 1$, we will see that phonon softening leads to $\lambda > \lambda_0$. The prescription for computing λ will be explained below in Eq.(9).

We investigate this model numerically via determinant quantum Monte Carlo (DQMC) simulations and analytically via ME theory. Details of the DQMC algorithm, including explanation of both the local and global phonon field updates used, can be found in [8]. Unless stated otherwise, we work with a square lattice with both nearestneighbor and next-nearest-neighbor hopping t'/t = -0.3and a fixed density n = 0.8. We keep a nonzero t' to avoid nesting near half-filling and also because previous studies have found that nonzero t' leads to an enhanced pairing response [9]. We have studied systems of linear size L=8-12 with periodic boundary conditions and temperatures $T = \beta^{-1} = t/4$ to t/16. All data in the main text is shown for our largest system size L = 12, which is large enough that most observables are essentially L independent, i.e. are characteristic of the thermodynamic limit. The DQMC results are shown as solid symbols in the various figures and where error bars are not visible, the statistical error is less than the symbol size. The figures also show comparisons of the DQMC results with ME theory, which is shown as either continuous curves or open symbols. ME calculations have also been carried out on system size L = 12. All data in the main text has the adiabatic ratio $\omega_0/E_F=0.1$, which puts us comfortably within the putative regime of validity of ME

theory. In the Supplemental Material we present data for other values of ω_0/E_F . We note that this model is free of the notorious minus-sign problem and hence we are able to access relatively large system sizes and low temperatures. However, for the parameters used here, we are still unable to access temperatures $T \lesssim t/16$ due to prohibitively long phonon autocorrelation times [10].

DQMC Results: While we typically cannot access sufficiently low temperatures to observe transitions to either a SC or a charge-density wave (CDW) phase, we do access low enough T that a significant growth of the corresponding susceptibilities can be measured, showing the ordering tendencies of the system. The s-wave pair susceptibility is defined as

$$\chi_{sc} = \int_0^\beta d\tau \ \langle \Delta(\tau) \Delta^{\dagger}(0) \rangle, \tag{4}$$

where

$$\Delta^{\dagger} = \frac{1}{L} \sum_{i} c_{i\uparrow}^{\dagger} c_{i\downarrow}^{\dagger}. \tag{5}$$

and the CDW susceptibility is

$$\chi_{cdw}(\mathbf{q}) = \int_0^\beta d\tau \ \langle \rho_{\mathbf{q}}(\tau) \rho_{\mathbf{q}}^{\dagger}(0) \rangle, \tag{6}$$

where

$$\rho_{\mathbf{q}}^{\dagger} = \frac{1}{L} \sum_{i,\sigma} e^{i\mathbf{q} \cdot \mathbf{R}_i} c_{i\sigma}^{\dagger} c_{i\sigma}. \tag{7}$$

We will use the symbol χ_{cdw} to represent the value of $\chi_{cdw}(\mathbf{q})$ evaluated at $\mathbf{q} \equiv \mathbf{Q}_{max}$ at which it is maximal.

In Figure 1 we plot χ_{sc} and χ_{cdw} as a function of λ_0 (lower axis) and λ (upper axis) at the lowest studied temperature $\beta t = 16$. The results from the ME theory, discussed in more detail in the next section, agree quantitatively with the data for $\lambda_0 \leq 0.4$ ($\lambda \lesssim 1.7$), after which the SC susceptibility takes a sharp downturn while the ME theory shows no similar features. We thus conclude that, for the parameters considered, ME theory breaks down dramatically for $\lambda_0 \gtrsim 0.4$. This is consistent with dynamical mean-field theory (DMFT) results reported by Bauer et al. [4]. Also evident from Fig. 1 is that the downturn in χ_{sc} is accompanied by a rapid rise of CDW correlations, which in turn leads to phonon softening and a corresponding increase in λ/λ_0 . We find that χ_{cdw} is peaked at wave-vector $\mathbf{Q}_{max} = (\pi, \pi)$ which, we emphasize, is a wave-vector not associated with any obvious features of the Fermi surface (see Inset of Fig. 3) for the Fermi surface). The abrupt nature of the breakdown of ME theory can also be seen in Fig. 2, where we plot χ_{sc} as a function of T for $\lambda_0 = 0.4, 0.5$ ($\lambda \approx 1.7, 4.6$). For $\lambda_0 = 0.4$, ME theory shows good agreement with the data over the entire temperature range $\beta t = 4-16$. However, for $\lambda_0 = 0.5$, while the ME theory does predict a

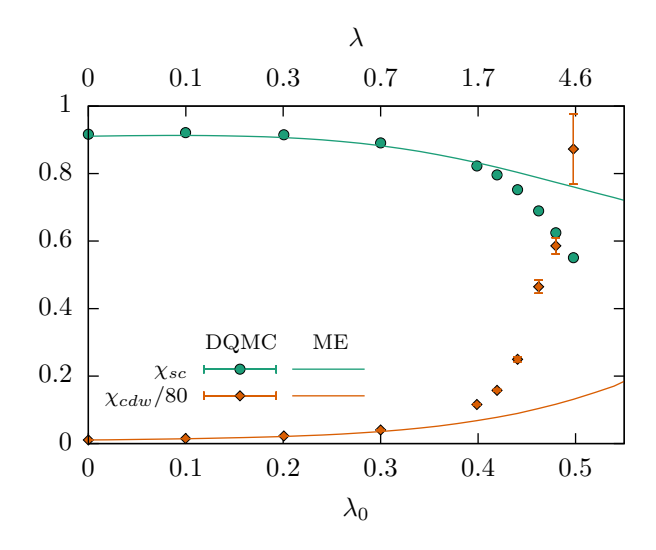


FIG. 1. χ_{sc} and χ_{cdw} as a function of λ_0 (lower scale) and λ (upper scale) for $\omega_0/E_F = 0.1$ at base temperature, $\beta t = 16$, density n = 0.8, and L = 12. Data points are DQMC values, solid lines are computed in ME approximation. We see a breakdown in the ME theory for $\lambda_0 \gtrsim 0.4$ ($\lambda \gtrsim 1.7$).

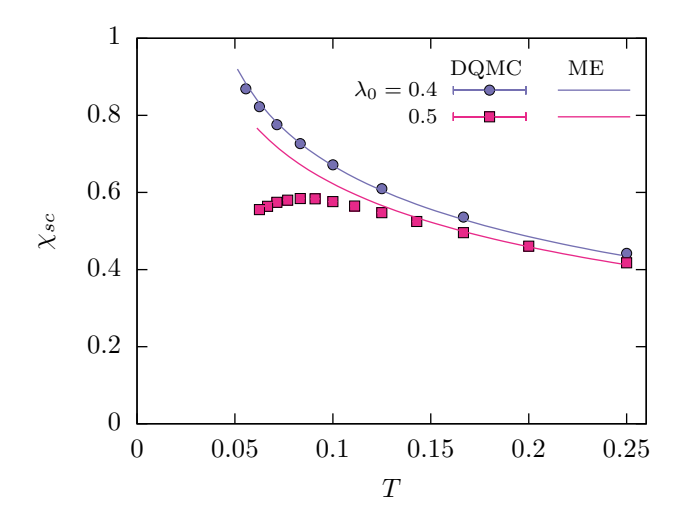


FIG. 2. χ_{sc} as a function of T for fixed values of $\lambda_0=0.4$ and 0.5 ($\lambda\approx 1.7$ and 4.6), $\omega_0/E_F=0.1$, n=0.8, and L=12. For $\lambda_0=0.4$, the ME theory accurately captures the behavior of χ_{sc} over the entire temperature range while for $\lambda_0=0.5$ the theory is qualitatively incorrect.

decrease in the pairing response relative to $\lambda_0 = 0.4$, it clearly misses even the qualitative behavior of χ_{sc} .

We have also computed the electron and phonon imaginary time ordered Green's functions. In Figure 3 we plot the imaginary part of the electronic self-energy $\text{Im}\Sigma$ for $\lambda_0 = 0.2, 0.4$, and 0.5 ($\lambda \approx 0.3, 1.7, 4.6$), as a function of Matsubara frequency $\omega_n = (2n+1)\pi T$ and for two momenta near the Fermi surface. For $\lambda_0 = 0.2$ the self-energy is nearly momentum independent and the Matsubara frequency dependence of $\text{Im}\Sigma$ is captured accu-

rately by ME theory. For $\lambda_0 = 0.4$ the self-energy develops weak momentum dependence and the dependence on both \mathbf{k} and ω_n is again captured well by ME theory. For $\lambda_0 = 0.5$ the self-energy remains weakly momentum dependent in both the ME and DQMC results but ME theory drastically underestimates the magnitude of the self-energy.

In Figure 4 we plot the renormalized phonon frequency $\Omega(\mathbf{q},0) = [\omega_0^2 + \Pi(\mathbf{q},0)]^{1/2}$, where $\Pi(\mathbf{q},\nu_n)$ is defined implicitly in terms of the phonon Green's function according to

$$D(\mathbf{q}, \nu_n) \equiv \frac{2\omega_0}{(i\nu_n)^2 - \omega_0^2 - \Pi(\mathbf{q}, \nu_n)}$$
(8)

and $\nu_n = 2\pi nT$. For $\lambda_0 = 0.2$ and 0.4 we see that the ME theory captures the renormalization of the phonon propagator with remarkable accuracy. (For $\lambda_0 = 0.4$, there is a noticeable error in the ME result in a narrow range of ${\bf q}$ around (π,π) ; this reflects an emerging problem in treating the CDW tendencies, as is discussed further in the Supplemental Material.) However, for $\lambda_0 = 0.5$, ME theory drastically underestimates (by a factor of ~ 3) the phonon softening at ${\bf q} = (\pi,\pi)$ and also gives a weaker softening near ${\bf q} = 0$.

Migdal-Eliashberg Theory: The ME theory for the normal state of an interacting e-p system can be summarized by the diagrams in Figure 5, which constitute a set of closed self-consistent equations for the electron and phonon self-energies. The approach is justified by the observation that the leading correction to the e-p vertex is proportional to ω_0/E_F , and hence can be ignored for $\omega_0/E_F \ll 1$ [1, 2]. As pointed out in [11], it is important to include self-consistently the equation for the phonon self-energy (rather than just using the bare phonon propagator in the electron self-energy equation) to account for effects due to phonon softening near a CDW transition. Details of the numerical procedure used to solve these equations and how the self-energies are used to compute various observables can be found in, e.g., [11, 12].

An important quantity entering the ME theory is the coupling constant λ [7], defined as

$$\lambda = 2 \int_0^\infty d\omega \, \frac{\alpha^2 F(\omega)}{\omega},\tag{9}$$

where $\alpha^2 F(\omega) = \rho(E_F) \alpha^2 \langle B(\mathbf{k} - \mathbf{k}', \omega) \rangle_{FS}$. Here $B(\mathbf{q}, \omega)$ is the phonon spectral function and the brackets denote the Fermi surface (FS) average

$$\langle B(\mathbf{k} - \mathbf{k}', \omega) \rangle_{FS} = \frac{1}{\rho(E_F)^2}$$
 (10)

$$\times \int \frac{d^2 \mathbf{k}}{(2\pi)^2} \frac{d^2 \mathbf{k}'}{(2\pi)^2} B(\mathbf{k} - \mathbf{k}', \omega) \delta(\epsilon_{\mathbf{k}} - E_F) \delta(\epsilon_{\mathbf{k}'} - E_F).$$

To extract this quantity from DQMC data we use the relationship between the imaginary time ordered phonon

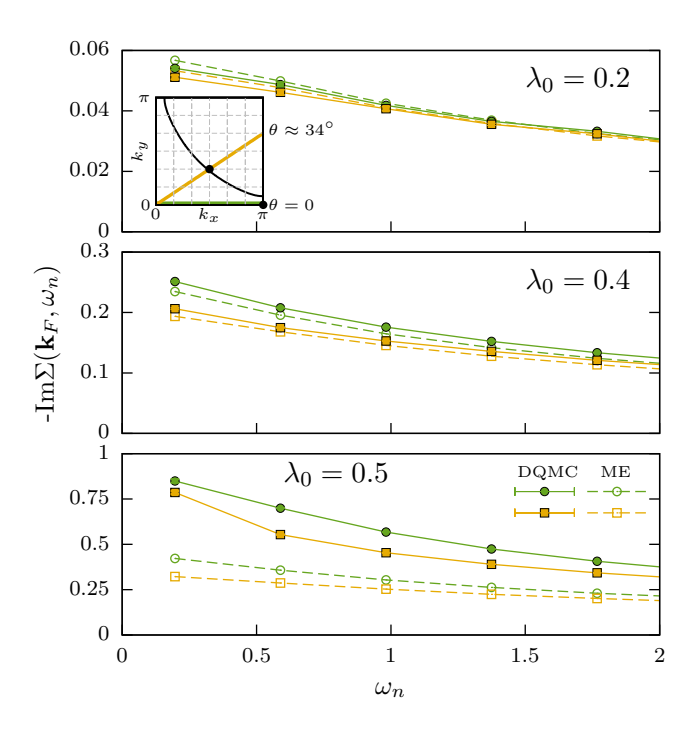


FIG. 3. Imaginary part of the electronic self energy, ${\rm Im}\Sigma({\bf k}\approx{\bf k}_F,\omega_n)$, where $\omega_n=(2n+1)\pi T$ and ${\bf k}\approx{\bf k}_F$ is a momentum near the Fermi surface, evaluated at $\theta=0$ and $\theta\approx34^\circ$. The inset shows the **k**-space mesh for an L=12 grid and the two points at which ${\rm Im}\Sigma$ is evaluated. These points correspond to the points closest to the zone diagonal and zone boundary respectively of the Fermi surface. The ME theory captures both the Matsubara frequency and momentum dependence of ${\rm Im}\Sigma$ for $\lambda_0\leq0.4$ but again shows a breakdown for $\lambda_0=0.5$. Other parameters are $\omega_0/E_F=0.1,\ \beta t=16,\ n=0.8,$ and L=12.

Green's function and the spectral function,

$$D(\mathbf{q}, \nu_n) = \int_0^\infty d\omega \ B(\mathbf{q}, \omega) \frac{2\omega}{(i\nu_n)^2 - \omega^2}, \qquad (11)$$

from which it follows that

$$\lambda = -\frac{\lambda_0 \omega_0}{2} \langle D(\mathbf{k} - \mathbf{k}', 0) \rangle_{FS}.$$
 (12)

Conclusions: Comparing the DQMC results on the Holstein model with ME theory, we find remarkably good quantitative agreement for e-p coupling less than a crossover value, $\lambda_0 \lesssim \lambda^* = 0.4$. However, as λ_0 exceeds λ^* , increasingly dramatic quantitative and qualitative differences develop. This is despite the fact that $\lambda(\bar{\Omega}/E_F)$ (the nominal control parameter for ME theory) is still small, and that the ME theory shows no sign that a crossover has occurred. (Note that while λ increases over λ_0 , the average phonon frequency $\bar{\Omega}$ decreases so that at $\lambda_0 = 0.5$, $\lambda \bar{\Omega}/E_F \approx 0.3$.) This crossover appears in some ways analogous to a first order transition – it involves a change in the character of the low energy theory to one which will eventually (at larger λ_0) be governed by

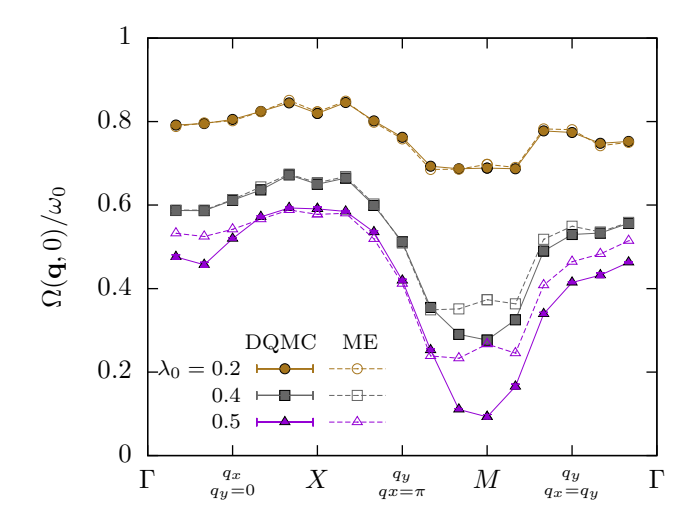


FIG. 4. Ratio of renormalized to bare phonon frequency. The renormalized phonon frequency is defined in Eq.(8). For $\lambda_0 \leq 0.4$ we see ME theory accurately predicts the momentum dependence of $\Omega(\mathbf{q},0)$. However, for $\lambda_0 = 0.5$, ME theory dramatically underestimates the softening of the phonon propagator at $\mathbf{q} = (\pi, \pi)$. Other parameters are $\omega_0/E_F = 0.1$, n = 0.8, $\beta t = 16$, and L = 12.

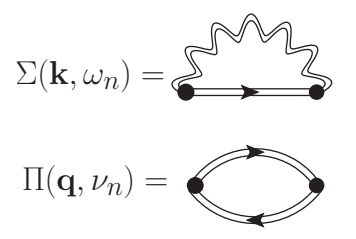


FIG. 5. Migdal equations for electronic and phonon self energies in the normal state. Double lines indicate fully renormalized Green's functions and the solid dot is the bare vertex α .

the strong-coupling physics of bipolarons, commensurate CDWs, and phase separation [3–5].

Our results are also interesting in the context of the quest for higher T_c superconductors. For $\lambda_0 \lesssim \lambda^*$, the measured χ_{sc} agrees well with ME theory in the accessible range of temperatures, and hence it is reasonable to use the ME expression as a way to extrapolate the DQMC results to lower T. By this line of reasoning, we can use the value of T_c computed within ME as a reliable estimate of the true T_c for λ_0 in this range. Since the ME T_c is an increasing function of λ_0 we conclude the same is true of the actual T_c , so long as $\lambda_0 \lesssim \lambda^*$. On the other hand, for $\lambda_0 = 0.5$ (where ME theory no longer agrees with the DQMC results), χ_{sc} from DQMC is a decreasing function of decreasing temperature (see Fig.2), from which we conclude T_c has been substantially suppressed and likely vanishes. This implies T_c is optimized around $\lambda_0 \approx \lambda^*$, where from ME theory we estimate that the

maximal T_c is $T_c^{(max)} \approx 8 \times 10^{-2} \omega_0$.

The property of an optimal T_c should be contrasted with conventional ME theory, which predicts a monotonically increasing T_c as a function of λ_0 [13, 14]. Of course, it is likely that the precise value of λ^* is nonuniversal, and there may be ways to engineer the model to increase it further - say by suppressing the CDW and/or polaronic tendencies. For instance, Pickett [15] has discussed the possibility of using multiple quasi-2D Fermi surfaces to enhance T_c and Werman and Berg [16] have recently shown that in a particular large N limit, in which the number of phonon modes is large compared to the number of fermionic modes, one can access the large λ limit without polaronic effects. However, as seen in H_3S [17, 18], it is probably a more promising route to increase T_c by increasing ω_0 (the prefactor in T_c) keeping $\lambda_0 \approx \lambda^*$, rather than increasing λ [19–21]. (On the other hand, increasing ω_0 makes the effects of bare Coulomb repulsion – which are completely absent in our treatment - more important.)

Finally, our results should be put in the context of previous studies of the Holstein model. The competition between SC and CDW has been studied via DQMC, albeit with a different focus and in a different parameter regime. (See [9, 11, 12, 22] and references therein.) The Holstein model has also been studied extensively via DMFT. (See [4, 23–28] for discussions of the crossover between weak and strong coupling as well as assessments of the validity of ME theory for the Holstein model.) The conclusions of these studies are broadly similar to those reached here. However, because the DMFT is done in infinite dimensions, we are unable to make quantitative comparisons with these studies. Using the dynamical cluster approximation (DCA), the inclusion of lowest-order vertex corrections has been studied [29]. In that study it was found that inclusion of vertex corrections tends to return the system to the ME regime by averting phonon softening. As we have seen, however, the ME theory already underestimates the phonon softening, suggesting that the inclusion of vertex corrections will not save the theory.

We would like to thank Akash Maharaj, Raghu Mahajan, and Abolhassan Vaezi for collaboration during early stages of this work. We acknowledge insightful discussions with Sri Raghu, Samuel Lederer, and Yoni Schattner. IE, BN, EWH, BM, and TPD were supported by the U.S. Department of Energy, Office of Basic Energy Sciences, Division of Materials Sciences and Engineering, under Contract No. DE-AC02-76SF00515. SAK was supported by NSF DMR-1608055. DJS was supported by the Scientific Discovery through Advanced Computing (SciDAC) program funded by U.S. Department of Energy, Office of Science, Advanced Scientific Computing Research and Basic Energy Sciences, Division of Materials Sciences and Engineering. This research was supported in part by the National Science Foundation under Grant No. NSF PHY11-25915. Computational work was performed on the SIMES and Sherlock clusters at Stanford University.

- [1] A. Migdal, Sov. Phys. JETP 7, 996 (1958).
- [2] G. Eliashberg, Sov. Phys. JETP 11, 696 (1960).
- [3] A. S. Alexandrov, EPL (Europhysics Letters) 56, 92 (2001).
- [4] J. Bauer, J. E. Han, and O. Gunnarsson, Phys. Rev. B 84, 184531 (2011).
- [5] E. W. Carlson, V. J. Emery, S. A. Kivelson, and D. Orgad, "Concepts in high temperature superconductivity," in *Superconductivity: Conventional and Unconventional Superconductors*, edited by K. H. Bennemann and J. B. Ketterson (Springer Berlin Heidelberg, Berlin, Heidelberg, 2008) pp. 1225–1348.
- [6] T. Holstein, Annals of Physics 8, 325 (1959).
- [7] P. B. Allen and B. Mitrović, in *Solid State Physics*, Vol. 37, edited by H. Ehrenreich, F. Seitz, and D. Turnbull (Academic Press, 1983) pp. 1 – 92.
- [8] S. Johnston, E. A. Nowadnick, Y. F. Kung, B. Moritz, R. T. Scalettar, and T. P. Devereaux, Physical Review B 87, 235133 (2013).
- [9] M. Vekić, R. M. Noack, and S. R. White, Phys. Rev. B 46, 271 (1992).
- [10] M. Hohenadler and T. C. Lang, in Computational Many-Particle Physics (Springer, 2008) pp. 357–366.
- [11] F. Marsiglio, Phys. Rev. B 42, 2416 (1990).
- [12] R. T. Scalettar, N. E. Bickers, and D. J. Scalapino, Phys. Rev. B 40, 197 (1989).
- [13] P. B. Allen and R. C. Dynes, Phys. Rev. B 12, 905 (1975).
- [14] V. Z. Kresin, Physics Letters A 122, 434 (1987).
- [15] W. E. Pickett, Journal of Superconductivity and Novel Magnetism 19, 291 (2006).
- [16] Y. Werman and E. Berg, Phys. Rev. B 93, 075109 (2016).
- [17] N. W. Ashcroft, Phys. Rev. Lett. 21, 1748 (1968).
- [18] A. P. Drozdov, M. I. Eremets, I. A. Troyan, V. Ksenofontov, and S. I. Shylin, Nature 525, 73 (2015).
- [19] C. Lin, B. Wang, and K. H. Teo, Phys. Rev. B 93, 224501 (2016).
- [20] C. Grimaldi, L. Pietronero, and S. Strässler, Phys. Rev. Lett. 75, 1158 (1995).
- [21] J. E. Han, O. Gunnarsson, and V. H. Crespi, Phys. Rev. Lett. 90, 167006 (2003).
- [22] R. M. Noack, D. J. Scalapino, and R. T. Scalettar, Phys. Rev. Lett. 66, 778 (1991).
- [23] J. K. Freericks, M. Jarrell, and D. J. Scalapino, Phys. Rev. B 48, 6302 (1993).
- [24] J. K. Freericks, Phys. Rev. B 48, 3881 (1993).
- [25] D. Meyer, A. C. Hewson, and R. Bulla, Phys. Rev. Lett. 89, 196401 (2002).
- [26] J. P. Hague and N. d'Ambrumenil, Journal of Low Temperature Physics 151, 1149 (2008).
- [27] P. Benedetti and R. Zeyher, Phys. Rev. B 58, 14320 (1998).
- [28] M. Capone and S. Ciuchi, Phys. Rev. Lett. 91, 186405 (2003).
- [29] J. P. Hague, Journal of Physics: Condensed Matter 15, 2535 (2003).

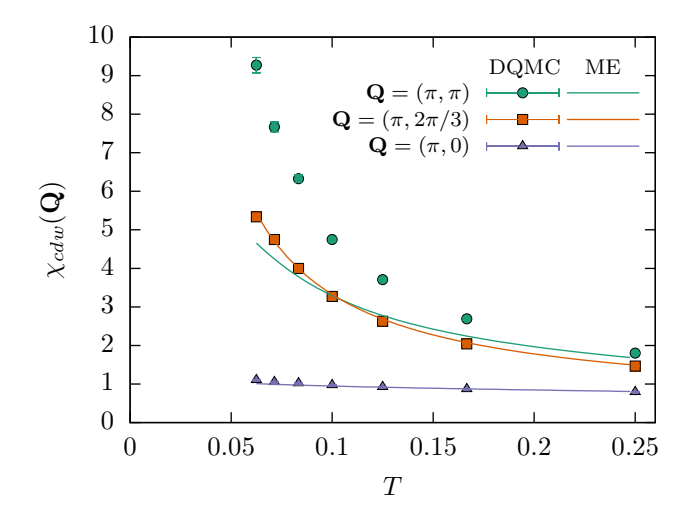


FIG. S1. χ_{cdw} as a function of T for three different wave-vectors \mathbf{Q} at coupling strength $\lambda_0 = 0.4$. See text for definitions of the different wave-vectors. Other parameters are $\omega_0/E_F = 0.1$, n = 0.8, and L = 12.

Supplementary Material: "Breakdown of Migdal-Eliashberg theory; a Quantum Monte Carlo study"

CDW DETAILS

Here we provide details on the charge-density-wave discussed in the main text. Parameters for all data discussed in this section are the same as those for data in the main text: nearest-neighbor and next-nearest-neighbor hopping t'/t = -0.3, density n = 0.8, and adiabatic ratio $\omega_0/E_F = 0.1$.

We focus on the case $\lambda_0=0.4$, which is roughly the largest coupling for which ME theory appears to be valid for the SC properties. Figure S1 compares the temperature evolution of $\chi_{cdw}(\mathbf{Q})$ from DQMC and ME theory, for three different wave-vectors $\mathbf{Q}=(\pi,\pi)$, $(\pi,2\pi/3)$, and $(\pi,0)$. These correspond, respectively, to the wave-vectors at which χ_{cdw} computed from DQMC is maximal, $\mathbf{Q}_{max}^{DQMC}=(\pi,\pi)$, at which the low T ME expression for the same quantity is maximal, $\mathbf{Q}_{max}^{ME}\approx(\pi,2\pi/3)$, and at a typical non-maximal \mathbf{Q} . Note that while \mathbf{Q}_{max}^{DQMC} is T independent, at elevated temperatures the ME expression for χ_{cdw} is maximal at (π,π) and only shifts to \mathbf{Q}_{max}^{ME} below $T\approx t/16$. As is already implicit in Fig. 4, ME theory correctly predicts the SC properties of the system for $\lambda_0=0.4$. Indeed, as can already be seen in Fig. 4, it correctly reproduces $\chi_{cdw}(\mathbf{Q})$ for most values of \mathbf{Q} . However, the ME expression produces unphysical peaks in χ_{cdw} at a \mathbf{Q} that is overly sensitive to the Fermi surface structure, and the peak value of χ_{cdw} is not as strongly divergent with decreasing T as the DQMC results. Both trends are, of course, much more dramatic for $\lambda_0=0.5$, as can be inferred from Fig. 4.

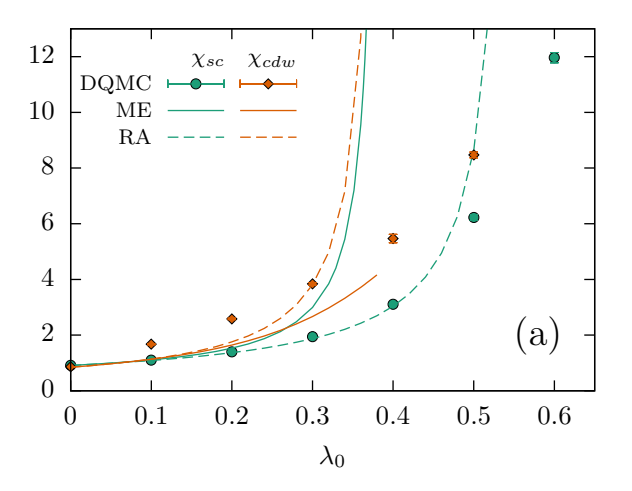
ADIABATIC RATIO $\omega_0/E_F=1$

In addition to the value of the adiabatic parameter $\omega_0/E_F = 0.1$ discussed in the main text, we have also studied $\omega_0/E_F = 1$. While this makes the nominal control parameter $\lambda_0\omega_0/E_F$ of ME theory larger, the larger phonon frequency also suppresses CDW ordering. The competition between an increase in the magnitude of vertex corrections and suppression of CDW ordering makes this an interesting regime in which to examine the validity of ME theory. In addition to the standard ME theory discussed in the main text, for this value of ω_0/E_F we also compare with a version of the ME equations in which the *bare* phonon propagator is used and only the electron self-energy is computed self-consistently. Because this approximation involves only the single rainbow diagram in Figure 5 of the main text, we call this the "rainbow approximation" (RA). This version of the approximation has often been used in the literature when assessing the validity of ME theory for the e-p problem [12, 22].

In Figure S2(a) we plot the SC and CDW susceptibilities χ_{sc} and χ_{cdw} as a function of λ_0 for fixed parameters $\omega_0/E_F = 1$, $\beta t = 16$, n = 0.8, and L = 12. We find the ME prediction for χ_{sc} begins to deviate from the DQMC

for $\lambda_0 \gtrsim 0.3$ and diverges shortly after, indicating a transition to a SC state. This is in contrast what was found for $\omega_0/E_F=0.1$, where the ME theory broke down for $\lambda_0\approx 0.4$ (see main text) and the breakdown correlated with a sharp increase in the growth of CDW correlations. On the other hand, the RA agrees well with the measured χ_{sc} up to $\lambda_0\approx 0.5$. We find that neither the standard ME approximation nor the RA provide accurate estimates of χ_{cdw} for $\lambda_0\gtrsim 0.1$.

In Figure S2(b) we plot χ_{sc} as a function of temperature for $\lambda_0 = 0.4$ and 0.6, with all other parameters the same as in Fig. S2(a). For $\omega_0/E_F = 0.1$ and $\lambda_0 = 0.4$, it was shown in the main text that ME theory captures χ_{sc} accurately over the entire temperature range. However, for $\omega_0/E_F = 1$ and $\lambda_0 = 0.4$, the ME prediction becomes inaccurate for $T \lesssim 0.1t$. On the other hand, the RA is accurate across the entire temperature range. For $\lambda_0 = 0.6$ the ME prediction becomes inaccurate at a temperature $T \approx 0.15t$, although the qualitative behavior is still correct. Based on the divergent behavior of χ_{sc} , the RA presumably predicts a SC transition temperature close to that predicted by the DQMC, although we have not attempted an accurate determination of T_c .



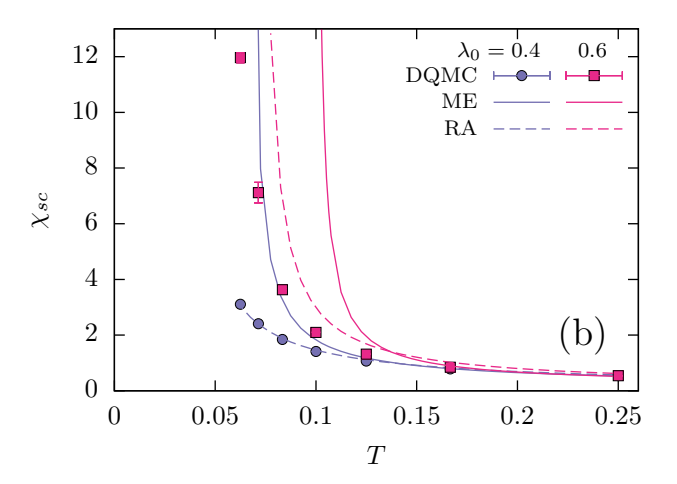


FIG. S2. (a) χ_{sc} and χ_{cdw} as a function of λ_0 for $\omega_0/E_F = 1$, $\beta t = 16$, n = 0.8, and L = 12. (b) χ_{sc} as a function of T for $\lambda_0 = 0.4$ and 0.6, with other parameters the same as in panel (a).